University of Groningen

Accuracy of Intraoperative Computed Tomography in Deep Brain Stimulation-A Prospective Noninferiority Study

Kremer, Naomi I; Oterdoom, D L Marinus; van Laar, Peter Jan; Piña-Fuentes, Dan; van Laar, Teus; Drost, Gea; van Hulzen, Arjen L J; van Dijk, J Marc C

IMPORTANT NOTE: You are advised to consult the publisher's version (publisher's PDF) if you wish to cite from it. Please check the document version below.

Document Version
Publisher's PDF, also known as Version of record

Link to publication in University of Groningen/UMCG research database

Accuracy of Intraoperative Computed Tomography in Deep Brain Stimulation—A Prospective Noninferiority Study

Naomi I. Kremer, BS* [iD] **; D. L. Marinus Oterdoom, MD*;**
Peter Jan van Laar, MD, PhD[†]; Dan Piña-Fuentes, MD*;
Teus van Laar, MD, PhD[‡]; Gea Drost, MD, PhD*[‡];
Arjen L. J. van Hulzen, MS[†]; J. Marc C. van Dijk, MD, PhD* [iD]

Introduction: Clinical response to deep brain stimulation (DBS) strongly depends on the appropriate placement of the electrode in the targeted structure. Postoperative MRI is recognized as the gold standard to verify the DBS-electrode position in relation to the intended anatomical target. However, intraoperative computed tomography (iCT) might be a feasible alternative to MRI.

Materials and Methods: In this prospective noninferiority study, we compared iCT with postoperative MRI (24-72 hours after surgery) in 29 consecutive patients undergoing placement of 58 DBS electrodes. The primary outcome was defined as the difference in Euclidean distance between lead tip coordinates as determined on both imaging modalities, using the lead tip depicted on MRI as reference. Secondary outcomes were difference in radial error and depth, as well as difference in accuracy relative to target.

Results: The mean difference between the lead tips was 0.98 ± 0.49 mm (0.97 ± 0.47 mm for the left-sided electrodes and 1.00 ± 0.53 mm for the right-sided electrodes). The upper confidence interval (95% CI, 0.851 to 1.112) did not exceed the noninferiority margin established. The average radial error between lead tips was 0.74 ± 0.48 mm and the average depth error was determined to be 0.53 ± 0.40 mm. The linear Deming regression indicated a good agreement between both imaging modalities regarding accuracy relative to target.

Conclusions: Intraoperative CT is noninferior to MRI for the verification of the DBS-electrode position. CT and MRI have their specific benefits, but both should be considered equally suitable for assessing accuracy.

Keywords: Accuracy, deep brain stimulation, intraoperative CT, movement disorders, stereotactic coordinates

Conflict of Interest: The authors report no conflict of interest concerning the materials or methods used in this study or the findings specified in this paper.

INTRODUCTION

Deep brain stimulation (DBS) is a well-recognized and effective neurosurgical treatment for various movement disorders. The clinical effect of DBS largely depends on the appropriate placement of the electrode in the targeted structure (1). Therefore, a correct assessment of the electrode position with imaging techniques during or directly after the surgical procedure is crucial, since it can timely indicate a necessary repositioning of the electrode.

Magnetic resonance imaging (MRI) is considered to be the gold standard to assess the electrode position after DBS implantation (2–9). MRI offers detailed visualization of relevant brain structures. However, image distortion caused by local magnetic field inhomogeneity may cause a nonconcentric artifact, usually larger than the electrode itself, which could possibly have a negative impact on the suitability of MRI for electrode position assessment (8,10,11).

Intraoperative computed tomography (iCT) offers a high spatial resolution and a good delineation of the DBS electrode, providing a precise localization of the electrode (12). CT is significantly cheaper (13) and less time consuming than MRI. Furthermore,

while iCT is readily available in most hospital settings, access to an intraoperative MRI is often limited.

Address correspondence to: Naomi I. Kremer, BS, University Medical Center Groningen, Hanzeplein 1 HPC AB71, Groningen 9713 GZ, the Netherlands. Email: n.i.kremer@umcg.nl

* Department of Neurosurgery, University of Groningen, University Medical Center Groningen, Groningen, The Netherlands;
† Department of Radiology, University of Groningen, University Medical Center Groningen, Groningen, The Netherlands; and
‡ Department of Neurology, University of Groningen, University Medical Center Groningen, Groningen, The Netherlands

A number of studies have been conducted regarding the most suitable imaging modality for assessing accuracy in DBS (10,14–16). However, these studies had several methodological limitations, such as nonconsecutive inclusions (10,16), only a retrospective character (10,15,16), uncertainty about the duration between CT and MRI scan (10,16) and the lack of sample size calculations (10,14–16).

This study was designed to compare iCT (fused with preoperative MRI (15,17–19)) with early postoperative MRI for electrode position verification in DBS surgery.

MATERIALS AND METHODS

Study Population and DBS Targets

We prospectively studied a single-institution series of 29 consecutive patients (mean age 58 ± 13.6 years, range: 16-76) undergoing bilateral DBS placement (58 electrodes) between November 2016 and April 2018. Thirty-eight electrodes were implanted in the subthalamic nucleus (STN), 14 in the internal globus pallidus (GPi), 4 in the zona incerta (ZI), and 2 in the thalamic ventral intermediate nucleus (VIM).

Imaging and Targeting

DBS targeting was based on preoperative 3 T MRI (Philips Intera, Eindhoven, the Netherlands), using the planning software iPlan 3.6 (Brainlab, Feldkirchen, Germany). Targeting was independently performed by two neurosurgeons. Preoperative stereotactic CT images (Sensation 64, Siemens, Erlangen, Germany) using the Leksell G frame (Elekta, Stockholm, Sweden) were transferred to the iPlan software and subsequently fused with the preoperative 3 T MRI to register the planned target in the stereotactic coordinate system. During the surgical procedure, immediately after bilateral lead placement, patients were brought to the Medical Imaging Unit, in which iCT images were obtained on a diagnostic CT suite (Sensation 64). A deviation from the intended target was manually calculated based on the iCT scan, using the iPlan probe view tool. If the lead was positioned <2 mm from the intended target, lead positioning was accepted. On the contrary, if a deviation of ≥2 mm off-target was determined, lead repositioning was performed immediately. Only one iCT verification was performed per patient. Afterwards, the internal pulse generator was implanted under general anesthesia. Within 24 to 72 hours after surgery, patients underwent 1.5 T-MRI (Aera, Siemens, Erlangen, Germany). Refer to Table 1 for imaging protocol specification.

The iCT and postoperative MRI datasets were fused to the preoperative stereotactic CT. The fusion of images by iPlan 3.6 runs automatically, using a mutual information algorithm for dataset correlation.

Lead Visualization and Localization

iPlan 3.6 was used to localize the leads. To improve visualization, a new trajectory was planned along the center of the lead artifact with a diameter of 1.2 mm, corresponding to the diameter of the actual lead (1.27 mm).

Lead artifacts appear differently on iCT and MRI (Fig. 1). An ellipsoid shaped artifact was seen on MRI, while a clear, well-delineated hyperdense artifact was seen on iCT. On iCT, a specific window level setting (Houndsfield Unit (HU) level: 1100 HU, width: 50 HU) was chosen to maximize contrast between lead and surrounding tissue, improving visualization. The lead position was determined as the imaginary center of the artifact on both modalities (Fig. 2). From the iCT and MRI datasets, the stereotactic coordinates of the lead tip were obtained, taking the most caudal part of the lead artifact as the lead tip position.

To study interobserver reliability, the plotting of the electrode trajectories was repeated by a neuroradiologist for all patients.

Direct Comparison Between Modalities: Euclidean Distance, Radial Error, and Depth

Lead tip coordinates were compared between both imaging modalities. The Euclidean distance between lead tip positions as determined on iCT and MRI was calculated for all electrodes.

$$Euclidean\ distance = \sqrt{(\Delta X^2 + \Delta Y^2 + \Delta Z^2)}$$

Besides the Euclidean distance, radial error and depth were assessed. Radial error is defined as the 2D distance in X and Y plane. For these assessments, the iCT lead was plotted into the postoperative MRI. Via the iPlan probe view tool, radial distance and depth were determined between the centers of both lead tips.

Indirect Comparison Between Modalities: Accuracy Relative to Target

Furthermore, the difference between both modalities and the intended target was determined. Targets were assessed according to the intended nucleus. The target is placed in the −1/+2 contact spacing of the DBS lead when the target is in the STN, VIM, or ZI, while in GPi stimulation, the intention is to insert the lead tip at target.

In the STN, VIM, ZI leads (44 leads), coordinates of the −1/+2 contact spacing of the DBS lead were calculated using vector

| Table 1. Imaging Protocol Specification.	
Imaging technique	**Scan protocol**
Preoperative 3 T MRI	3D T1, 200 slices, slice distance 0.9 mm + T2, axial, coronal and sagittal planes, 30 slices, slice distance 2 mm, matrix size: 260 × 320 × 160, voxel size: 0.75 mm × 0.75 mm × 1 mm
Preoperative CT	Axial planes, 2 mm slice distance, 60 slices, matrix size: 512 × 512 × 64, voxel size: 0.488 mm × 0.488 mm × 2 mm
Intraoperative CT	Axial planes, 0.5 mm slice distance, 270 slices with image reconstruction for brain parenchyma and (early) hematoma assessment (5 mm connecting slices using the soft tissue algorithm), matrix size: 512 × 512 × 297, voxel size: 0.488 mm × 0.488 mm × 0.5 mm
Postoperative 1.5 T MRI	Axial and coronal planes, 30 and 15 slices respectively, 2.2 mm slice distance, matrix size: 290 × 320 × 27, voxel size: 0.719 mm × 0.719 mm × 2.2 mm
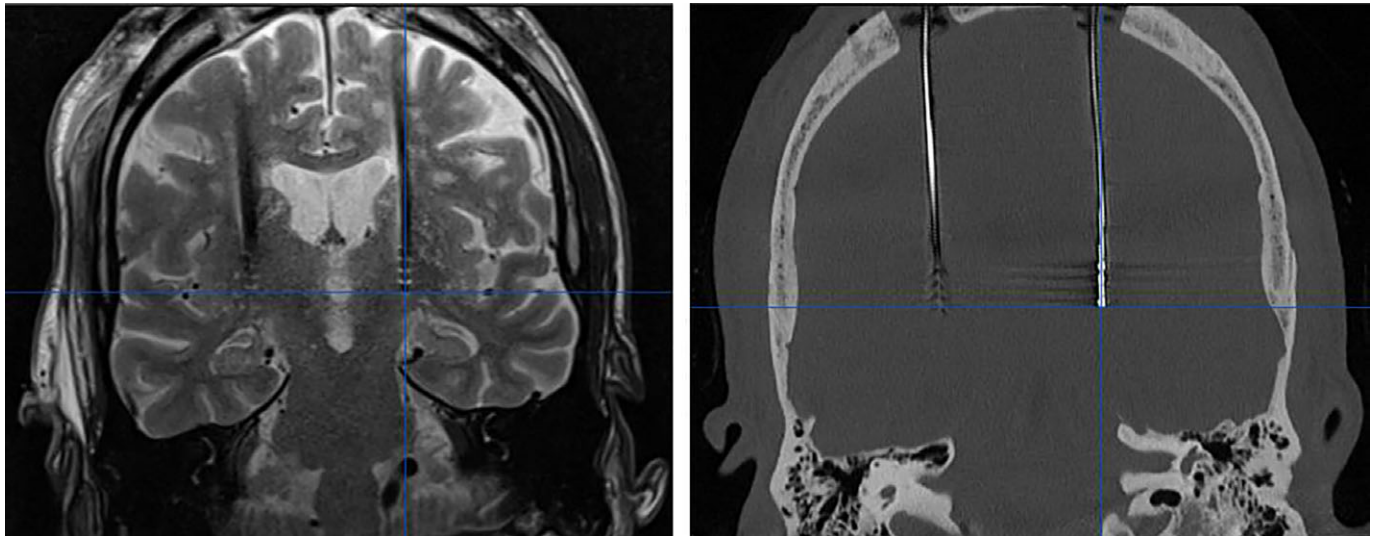
Figure 1. DBS leads of the same patient on MRI (left) and on iCT (before windowing; right). The MRI artifact is depicted as a hypodense signal whereas the CT artifact is hyperdense. [Color figure can be viewed at wileyonlinelibrary.com]

geometry. The Euclidean distance between these coordinates and the intended target coordinates were calculated, using the aforementioned formula.

In the GPi leads (14 leads), the Euclidean distance between the lead tip coordinates and the intended target coordinates were calculated.

Statistical Analysis

The primary hypothesis was that iCT would be noninferior to postoperative MRI for the verification of the DBS lead position. We determined a noninferiority margin of 2 mm. It has been described in literature (20–22) that the weighted mean distance between lead tips on CT and MRI is 1.50 ± 0.50 mm. Accordingly, we estimated a difference of 0.50 mm or more to be clinically

relevant for the accuracy estimation. To calculate our sample size, we used a Cohen's d (mean difference/standard deviation, d) of 1. Based on a power $(1 - \beta)$ of 0.95 and an alpha significance level (α) of 0.025, we estimated that 16 electrode distances were needed for our statistical analysis.

Calculations were performed according to the formula (23):

$$n\,(\text{number of electrodes}) = f(\alpha, \beta) \times 2 \times \sigma^2 / d^2$$

In which f is the function of α and β, σ is the standard deviation, and d is the noninferiority limit.

Thus, 29 participants implanted with 58 electrodes had sufficient power determine the possible noninferiority of iCT to MRI.

Euclidean distances resulted from the direct comparison of iCT and MRI leads, were compared with the mean distance previously
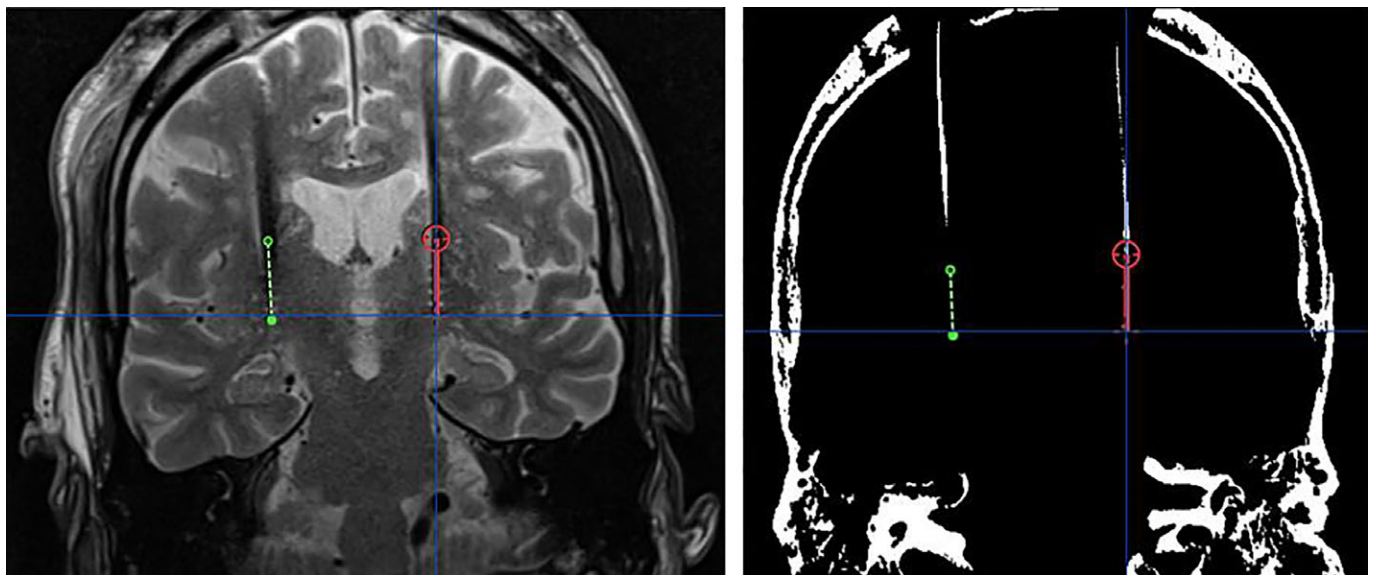

Figure 2. Lead visualization and plotted lead trajectory on MRI (left) and iCT (after windowing; right) in the same patient using the *probe view* in iPlan. The red and green lines represent the left-sided and the right-sided lead-artifact, respectively. [Color figure can be viewed at wileyonlinelibrary.com]

3

reported in literature using a one sample right-tailed *t*-test. Confidence intervals (CIs) were calculated to determine whether the upper limit of the CI exceeded the noninferiority margin.

For the indirect comparison between modalities, a linear Deming regression was performed between the error from target to lead in Euclidean distance, estimated both using MRI and CT. The variances were assumed to be similar between both modalities (lambda = 1) and the level of significance alpha was determined at 0.05. The correlation between both techniques was estimated using Pearson's *r*.

The statistical analysis was performed using R version 3.5.1 and the statistical package mcr. Descriptive statistics are given with mean and standard deviation. Intraclass correlation (ICC) with 95% CI were obtained for two raters for interobserver reliability.

According to Dutch legislation, the local research ethical board stated that the study was not submitted to the Medical Research Involving Human Subjects Act (WMO).

RESULTS

Direct Comparison Between Modalities: Euclidean Distance, Radial Error, and Depth

In our cohort, one lead position was revised after initial implantation because the lead was placed 2 mm too superficial as determined on iCT. After placing the lead 2 mm more caudal, an additional iCT was not acquired. Therefore, this lead was excluded and analysis was performed in 57 leads. The average Euclidean distance between lead tips was 0.98 ± 0.49 mm; 0.97 ± 0.47 mm for the left-sided electrode and 1.00 ± 0.53 mm for the right-sided electrode (Table 2). The calculated mean Euclidean distances were not significantly higher than the reported weighted mean ($t_{56} = -7.9335$, $p = 1$). The upper CI (0.851-1.112) did not exceed the noninferiority margin established.

The average radial error between lead tips was 0.74 ± 0.48 mm, whereas the average depth error was determined to be 0.53 ± 0.40 mm.

Indirect comparison between modalities: accuracy relative to target

On iCT, the average Euclidean distance between the DBS lead and the intended target was 1.71 ± 0.61 mm; 1.98 ± 0.61 mm for the left-sided electrode and 1.40 ± 0.45 mm for the right-sided electrode.

Table 2. Absolute Differences Between Lead Tip Coordinates on iCT and Postoperative MRI.

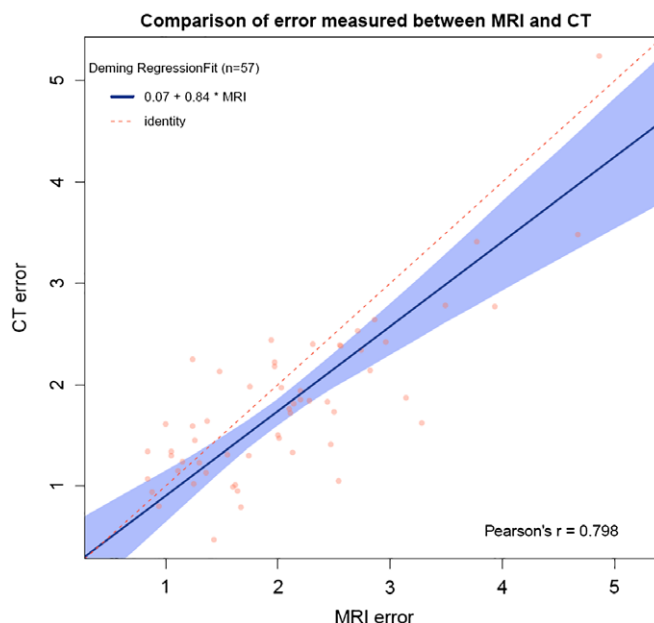|		Average ± SD (mm)	Range (mm)
All leads	Euclidean distance	0.98 ± 0.49	0.14-2.58
	X	0.35 ± 0.25	0.00-1.20
	Y	0.61 ± 0.52	0.00-2.50
	Z	0.49 ± 0.39	0.00-1.80
Left lead	Euclidean distance	0.97 ± 0.47	0.36-2.58
	X	0.33 ± 0.21	0.00-0.80
	Y	0.59 ± 0.53	0.00-2.50
	Z	0.51 ± 0.34	0.00-1.20
Right lead	Euclidean distance	1.00 ± 0.53	0.14-2.04
	X	0.36 ± 0.29	0.00-1.20
	Y	0.63 ± 0.51	0.00-2.00
	Z	0.47 ± 0.44	0.10-1.80

Figure 3. Linear Deming regression plot indicating good agreement between iCT and MRI. [Color figure can be viewed at wileyonlinelibrary.com]

On MRI, the average Euclidean distance between the DBS lead and the intended target was 1.94 ± 0.74 mm; 2.19 ± 0.61 mm for the left-sided electrode and 1.70 ± 0.79 mm for the right-sided electrode.

The linear Deming regression indicated a good agreement between both imaging modalities (intercept 0.066, CI −0.3607 to 0.5310, slope 0.08362, CI 0.6047 to 1.0326). The CI of the intercept contains 0, which indicates no significant accuracy difference between CT and MRI, while the CI of the slope contains 1, which indicates no significant difference in the precision of both imaging techniques. Pearson's *r* was 0.798, showing a strong correlation between both MRI and CT (Fig. 3).

Intraclass Correlations

The lead tip two-rater interobserver ICC showed an almost perfect agreement for both iCT and MRI measurements, 0.999 (95% CI; range: 0.699-1.000) and 0.995 (95% CI; range: 0.940-0.998), respectively.

DISCUSSION

Ideally, proper visualization of the DBS lead and the nucleus borders of the target would either ensure correct lead position or shed light upon the need for revision. Unfortunately, the current imaging techniques have not reached the stage in which both DBS lead and nucleus borders can be clearly visualized. MRI offers detailed visualization of relevant brain structures, but also induces an artifact that overestimates the actual electrode. Besides, DBS systems are not always compatible with MRI and occurrence of adverse events have been described in DBS implanted patients after MRI (24). Also, the specific absorption rate limits implemented in MRI safety protocols as a result of these concerns can limit the quality of the images (depending on sequence), resulting in suboptimal images for lead verification. In addition, access to an intraoperative MRI suite is limited in most hospitals. All the more reason for the entry of an alternative imaging modality in DBS surgery.

Our study shows that iCT is noninferior to MRI for the verification of lead position in DBS surgery. The average Euclidean distance between lead tip position determined on iCT and MRI was 0.98 mm ± 0.49 mm, which is lower than the noninferiority margin for significant clinical relevance.

The differences found in this study are smaller than those found in other studies on lead localization in DBS. Shahlaie et al. (20) found differences of 1.65 ± 0.19 mm between lead tips on iCT and postoperative MRI. Based on the conclusions of previous publications (16,18,20) and the results obtained in this article, the authors agree that iCT could replace postoperative MRI in assessing DBS leads. Lee et al. (10) directly fused postoperative CT and postoperative MRI and subsequently compared the lead centers at five different levels. The lead centers showed differences of 1.08 mm to 1.40 mm. Thani et al. (22) performed intraoperative MRI with a surrogate marker (carbothane stylette, in which the lead was placed later) and fused this dataset with postoperative CT (with DBS electrodes) to calculate the discrepancy between the location of the active contact of the two images. The discrepancy found was 1.60 ± 0.20 mm. Carlson et al. (21) reported a distance of 1.43 ± 0.66 mm comparing postoperative MRI (1-2 weeks) and postoperative CT (12 hours).

Besides studying the difference of the lead tip position on iCT and MRI, the difference between the lead and the intended target was assessed on each modality, because this information is very important for the intraoperative decision to revise the lead or not. Larger Euclidean distances were found between target and DBS lead on MRI, compared to iCT (1.94 ± 0.74 mm vs. 1.71 ± 0.61 mm). This difference between modalities is most likely caused by the difficulty both lead tip assessors experienced identifying the lead tip on MRI. The often unclear black artifact was not well-delineated and showed a gradual beginning at the lead tip, making it difficult to accurately mark the lead tip. Difficulty visualizing the lead tip on MRI imaging has been described before (16,18).

Assessing Lead Position Based on Artifact Visualization

On both CT and MRI the electrode induces an artifact that exceeds the actual electrode size. To accurately assess lead positioning on imaging, it is important to exactly know the electrode position in relation to the artifact. On MRI, DBS leads are depicted as ellipse-shaped low signal artifacts, in which each contact point individually induces a symmetrical artifact extending approximately 1.4 mm over the proximal and distal ends of the contact and 1.16 mm over the lateral limit of the contact (11). This suggests that both the artifact and the relative contact have the same center (8,11). Pollo et al. thus identified 1.4 mm to be the distance on MRI between the distal limit of the artifact and the distal limit of the first contact (contact 0). On CT, lead artifacts appear as a clear, hyperdense signal in the darkened (after windowing) intracranial space. Because of the high spatial fidelity of CT, the artifact is likely to be concentrically formed around the lead (25). Hemm et al. conducted a study based on lead artifacts on CT images and found distances of 1.1 mm and 1.2 mm between the beginning of the artifact and the distal limit of contact 0, in their *in vivo* and *in vitro* study, respectively (12). In our study, the above cited distances were taken into account when calculating the exact position of the −1/+2 contact spacing for assessing the lead position relative to target.

Limitations

The position of the lead tip and the lead position relative to the target was compared between modalities, taken into account the imaging specific characteristics of the different lead artifacts. However, since the distance from lead tip to contact 0 varies between MRI and CT (1.4 mm vs. 1.2 mm), contact 0 might be more suitable than the lead tip to compare modalities. Nonetheless, the lead tip has been extensively used to study accuracy in the past (26–29) and a difference of 0.2 mm between modalities is very small.

Fusion error could have played a role in the accuracy of lead measurements. When fusion between imaging sets was being performed, fusion was always visually verified by checking ventricular and sulcal shape. In none of the cases manual fusion adjustment was necessary.

Another limitation in our study might be the difference in time between the iCT and the postoperative MRI (24–72 hours). Ideally, the postoperative MRI should be performed directly after the iCT to minimize any effects related to brain shift, but this was not possible because of logistic reasons. Therefore, brain shift could have led to a less reliable comparison between both imaging modalities.

Future Perspectives

The results show that iCT is noninferior to postoperative MRI for lead localization in DBS surgery. Our institution may therefore have the possibility of proceeding towards an asleep DBS procedure using iCT, since iCT proves to measure up to the gold standard, MRI. Good results have been published by recent studies regarding asleep DBS surgery (30–38). Asleep DBS is proven to be safe and without differences in adverse events compared to awake DBS (33). The asleep procedure could possibly be even more effective (35) and may be cheaper (39) than operating in an awake situation. Risk of surgical complications such as hemorrhages or infections are also significantly less frequent in asleep DBS (32,37).

In the current study, we have proven iCT to be noninferior to postoperative MRI, whereby our surgical group can advance to performing asleep surgery in our patients using iCT. The lack of MRI availability does not hinder the possibility to perform asleep DBS surgery.

CONCLUSION

In this prospective study iCT was found to be noninferior to postoperative MRI for the verification of the lead position in DBS surgery. There were no relevant differences between the lead position on iCT and postoperative MRI. In conclusion, both modalities have their pros and cons, but either one is suitable for lead position verification in DBS surgery.

Authorship Statements

REFERENCES

1. Ellis TM, Foote KD, Fernandez HH et al. Reoperation for suboptimal outcomes after deep brain stimulation surgery. *Neurosurgery* 2008;63:754–760.
2. Matias CM, Frizon LA, Asfahan F, Uribe JDMA. Brain shift and Pneumocephalus assessment during frame-based deep brain stimulation implantation with intraoperative magnetic resonance imaging. *Oper Neurosurg.* 2018;14:668–674.
3. Martin AJ, Starr PA, Ostrem JL, Larson PS. Hemorrhage detection and incidence during magnetic resonance-guided deep brain stimulator implantations. *Stereotact Funct Neurosurg* 2017;95:307–314.
4. Liu X, Zhang J, Fu K, Gong R, Chen J, Zhang J. Microelectrode recording–guided versus intraoperative magnetic resonance imaging–guided subthalamic nucleus deep brain stimulation surgery for Parkinson disease: a 1-year follow-up study. *World Neurosurg* 2017;107:900–905.
5. Breit S, Lebas JF, Koudsie A, Schulz J, Benazzouz A, Pollak PBA. Pretargeting for the implantation of stimulation electrodes into the subthalamic nucleus: a comparative study of magnetic resonance imaging and ventriculography. *Oper Neurosurg* 2006;58:ONS83–ONS95.
6. Counelis GJ, Simuni T, Forman MS, Jaggi JL, Trojanowski JQBG. Bilateral subthalamic nucleus deep brain stimulation for advanced PD: Correlation of intraoperative MER and postoperative MRI with neuropathological findings. *Mov Disord* 2003;18:1062–1065.
7. Pinto S, Le Bas JF, Castana L, Krack P, Pollak PBA. Comparison of two techniques to postoperatively localize the electrode contacts used for subthalamic nucleus stimulation. *Neurosurgery* 2007;60:285–292. discussion 292-4.
8. Pollo C, Vingerhoets F, Pralong E et al. Localization of electrodes in the subthalamic nucleus on magnetic resonance imaging. *J Neurosurg* 2007;106:36–44.
9. Hyam JA, Akram H, Foltynie T, Limousin P, Hariz M, Zrinzo L. What you see is what you get: lead location within deep brain structures is accurately depicted by stereotactic magnetic resonance imaging. *Clin Neurosurg* 2015;11:412–419. discussion 419.
10. Lee JY, Kim JW, Lee JY et al. Is MRI a reliable tool to locate the electrode after deep brain stimulation surgery? Comparison study of CT and MRI for the localization of electrodes after DBS. *Acta Neurochir* 2010;152:2029–2036.
11. Pollo C, Villemure JG, Vingerhoets F et al. Magnetic resonance artifact induced by the electrode Activa 3389: an in vitro and in vivo study. *Acta Neurochir* 2004;146:161–164.
12. Hemm S, Coste J, Gabrillargues J et al. Contact position analysis of deep brain stimulation electrodes on post-operative CT images. *Acta Neurochir* 2009;151:823–829.
13. O'Neill BR, Pruthi S, Bains H et al. Rapid sequence magnetic resonance imaging in the assessment of children with hydrocephalus. *World Neurosurgery* 2013;80:e307–e312.
14. Pinsker MO, Herzog J, Falk D, Volkmann J, Deuschl G, Mehdorn M. Accuracy and distortion of deep brain stimulation electrodes on postoperative MRI and CT. *Zentralbl Neurochir* 2008;69:144–147.
15. Xia J, He P, Cai X, Zhang D, Xie N. Magnetic resonance and computed tomography image fusion technology in patients with Parkinson's disease after deep brain stimulation. *J Neurol Sci* 2017;381:250–255.
16. Bot M, van den Munckhof P, Bakay R, Stebbins G, Verhagen Metman L. Accuracy of intraoperative computed tomography during deep brain stimulation procedures: comparison with postoperative magnetic resonance imaging. *Stereotact Funct Neurosurg* 2017 Jun 10 [cited 2017 Jun 25];95:183–8. Available from: http://www.ncbi.nlm.nih.gov/pubmed/28601874
17. Geevarghese R, Ogorman Tuura R, Lumsden DE, Samuel M, Ashkan K. Registration accuracy of CT/MRI fusion for localisation of deep brain stimulation electrode position: an imaging study and systematic review. *Stereotact Funct Neurosurg* 2016;94:159–163.
18. Mirzadeh Z, Chapple K, Lambert M, Dhall R, Ponce FA. Validation of CT-MRI fusion for intraoperative assessment of stereotactic accuracy in DBS surgery. *Mov Disord* 2014;29:1788–1795.
19. O'Gorman RL, Jarosz JM, Samuel M, Clough C, Selway RP, Ashkan K. CT/MR image fusion in the postoperative assessment of electrodes implanted for deep brain stimulation. *Stereotact Funct Neurosurg* 2009;87:205–210.
20. Shahlaie K, Larson PS, Starr PA. Intraoperative computed tomography for deep brain stimulation surgery: technique and accuracy assessment. *Neurosurgery* 2011;68:114–124. discussion 124.
21. Carlson JD, McLeod KE, McLeod PS, Mark JB. Stereotactic accuracy and surgical utility of the O-arm in deep brain stimulation surgery. *Oper Neurosurg* 2017;1:96–107.
22. Thani NB, Bala A, Swann GB, Lind CRP. Accuracy of postoperative computed tomography and magnetic resonance image fusion for assessing deep brain stimulation electrodes. *Neurosurgery* 2011;69:207–214.
23. Sealed Envelope Ltd. 2012. Power calculator for continuous outcome non-inferiority trial. [Online] Available from: https://www.sealedenvelope.com/power/continuous-noninferior/.
24. Henderson JM, Tkach J, Phillips M, Baker K, Shellock FG, Rezai AR. Permanent neurological deficit related to magnetic resonance imaging in a patient with implanted deep brain stimulation electrodes for Parkinson's disease: case report. *Neurosurgery* 2005 Nov [cited 2018 Oct 23];57:E1063; discussion E1063. Available from: http://www.ncbi.nlm.nih.gov/pubmed/16284543
25. Sumanaweera TS, Adler JR Jr, Napel S, Glover GH. Characterization of spatial distortion in magnetic resonance imaging and its implications for stereotactic surgery. *Neurosurgery* 1994;35:696–703. discussion 703–4.
26. Daniluk S, Davies KG, Novak P, Vu T, Nazzaro JM, Ellias SA. Isolation of the brain-related factor of the error between intended and achieved position of deep brain stimulation electrodes implanted into the subthalamic nucleus for the treatment of Parkinson's disease. *Neurosurgery* 2009;64(5 Suppl 2):374–3782; discussion 382–384.
27. McClelland S, Ford B, Senatus PB et al. Subthalamic stimulation for Parkinson disease: Determination of electrode location necessary for clinical efficacy. *Neurosurg Focus* 2005;19:E12.
28. Ferroli P, Franzini A, Marras C, Maccagnano E, D'Incerti L, Broggi G. A simple method to assess accuracy of deep brain stimulation electrode placement: preoperative stereotactic CT + postoperative MR image fusion. *Stereotact Funct Neurosurg* 2004;82:14–19.
29. Lumsden DE, Ashmore J, Charles-Edwards G, Lin JP, Ashkan K, Selway R. Accuracy of stimulating electrode placement in paediatric pallidal deep brain stimulation for primary and secondary dystonia. *Acta Neurochirurgica* 2013;155:823–836.
30. Mirzadeh Z, Chapple K. Parkinson's disease outcomes after intraoperative CT-guided "asleep" deep brain stimulation in the globus pallidus internus. *J Neurosurg* 2016;124:902–907.
31. Chen T, Mirzadeh Z, Chapple K, Lambert M, Dhall RPF. "Asleep" deep brain stimulation for essential tremor. *J Neurosurg* 2016;124:1842–1849.
32. Ho AL, Ali R, Connolly ID et al. Awake versus asleep deep brain stimulation for Parkinson's disease: a critical comparison and meta-analysis. *J Neurol Neurosurg Psychiatry* 2018;89:687–691.
33. Chen T, Mirzadeh Z, Chapple K, Lambert M, Ponce FA. Complication rates, lengths of stay, and readmission rates in "awake" and "asleep" deep brain stimulation. *J Neurosurg* 2017;127:360–369.
34. Chen T, Mirzadeh Z, Ponce FA. "Asleep" deep brain stimulation surgery: a critical review of the literature. *World Neurosurg* 2017;105:191–198.
35. Brodsky MA, Anderson S, Charles Murchison P et al. Clinical outcomes of asleep vs awake deep brain stimulation for Parkinson disease. *Neurology* 2017;89:1944–1950.
36. Chen T, Mirzadeh Z, Chapple KM et al. Clinical outcomes following awake and asleep deep brain stimulation for Parkinson disease. *J Neurosurg* 2018;16:1–12.
37. Warnke PC. Deep brain stimulation surgery under general anaesthesia with microelectrode recording: the best of both worlds or a little bit of everything? *J Neurol Neurosurg Psychiatry* 2014;85:1063.
38. Ko AL, Magown P, Ozpinar A, Hamzaoglu V, Burchiel KJ. Asleep deep brain stimulation reduces incidence of intracranial air during electrode implantation. *Stereotact Funct Neurosurg [Internet]* 2018;96:83–90. Available from:. www.karger.com/sfn.
39. Jacob RL, Geddes J, McCartney S, Burchiel KJ. Cost analysis of awake versus asleep deep brain stimulation: A single academic health center experience. *J Neurosurg* 2016;124:1517–1523.